Frequency-Resolved Coherent LIDAR using a Femtosecond Fiber Laser

W. C. Swann and N. R. Newbury
National Institute of Standards and Technology, 325 Broadway, Boulder, CO 80305
email: nnewbury@boulder.nist.gov, phone: 303-497-4227, fax: 303-497-3387

Abstract: We present a frequency comb-based, frequency-resolved coherent LIDAR (FReCL) that provides higher performance than that of conventional pulsed range/Doppler LIDARs, dramatically reduces local oscillator timing requirements, and compensates for path dispersion.

OCIS codes: (140.3510) Lasers, Fiber; (280.3640) Lidar; (120.0280) Remote sensing

Femtosecond frequency combs provide a broadband coherent light source that has revolutionized optical frequency metrology [1]. Extending their use to coherent light detection and ranging (CLIDAR) is natural, since the broad spectrum supports high range resolution, and each comb tooth's narrow linewidth supports high Doppler resolution. Moreover, fiber combs at 1.5 μm [2, 3] are compatible with high-power erbium-doped fiber amplifiers. Frequency combs have already been employed in a ranging LIDAR [4] and proposed for a space-based ranging LIDAR [5]. However, wide bandwidth CLIDAR reflecting from a remote rough surface poses several difficulties. First, the return signal will suffer from speckle, which limits the signal-to-noise ratio to unity regardless of the transmitted power, and which broadens the frequency spectrum to the speckle bandwidth, reducing the sensitivity to Doppler shifts. Second, achieving the high range resolution afforded by the wide bandwidth requires excellent control of a variable delay line and negligible differential dispersion between the local oscillator (LO) and signal arms.

To address these issues, we demonstrate a Frequency-Resolved Coherent LIDAR (FReCL) [6]. In FReCL, the heterodyne signal is spectrally resolved into N channels and then processed. Our system differs from previous frequency-comb LIDARs and shares features of Fourier-Domain Optical Coherence Tomography [7] and speckle-averaging CLIDARs [8, 9]. It provides N-times improvement in acquisition time, reduces the requirements of the variable delay, and compensates for differential dispersion between the signal and LO arms.

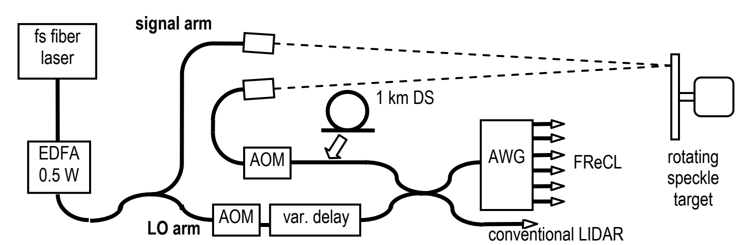

Fig. 1. System layout. Solid lines are optical fiber paths, dotted lines are air paths. The variable delay line precisely adjusts the relative delay between the two arms and allows scanning the conventional LIDAR's range. The heterodyne signal runs to the six FReCL detectors and to the single conventional LIDAR detector. 1 km of dispersion-shifted (DS) fiber added to the signal arm demonstrates operation with unequal path lengths and dispersion. AOM: acousto-optic modulator.

The setup is shown in Fig. 1. The signal beam hits the edge of a rough target rotating at about 10 Hz, resulting in a speckle bandwidth of ~2-15 kHz depending on target tilt. The LO arm is equal to the signal arm modulo the laser repetition rate of 50 MHz. Alternatively, a second phase-locked fiber comb can serve as a phase-locked LO to remove this restriction [10]. The signal bandwidth of λ_{BW} =25 nm is sampled directly in the conventional channel, but is spectrally filtered in the FReCL channels. Here we sparsely sampled the return with N=6 discrete detectors evenly spaced by λ_{sp}=4.8 nm, resulting in a range ambiguity of $\lambda^2/(2\lambda_{sp}) \sim 250$ μm, but retaining the full range resolution of $\lambda^2/(2\lambda_{BW}) \sim 50$ μm. The AOMs were adjusted to generate a heterodyne signal at ~30 kHz, which was processed in software to generate a signal for the n[th] channel, $V_n(t)$. The FReCL signals are processed coherently to generate a range image or incoherently to generate a Doppler signature of the target.

To generate an image, we construct a range gate at a virtual delay τ by $V(t,\tau) = \sum V_n(t)\exp(i2\pi\Delta\nu n\tau)$, where Δν is the channel spacing and $\Delta\nu n\tau_\kappa$ is a phase shift added to the n^{th} channel. Figure 2a shows a conventional CLIDAR image taken with fine (0.1 ps) steps of the delay line. A wobble of ~100 μm in the disk position is evident (and was confirmed by mechanical measurement). Figure 2b shows the single stripe of data available from the conventional channel in one target rotation, while Fig. 2c shows the image acquired by the FReCL data at the same *single* fixed delay. Figure 3 shows a similar data set where the signal path was increased by 1 km of fiber. Dispersion completely destroys the resolution of the conventional channel, while through phase compensation applied in processing [7], the resolution is restored for the FReCL data.

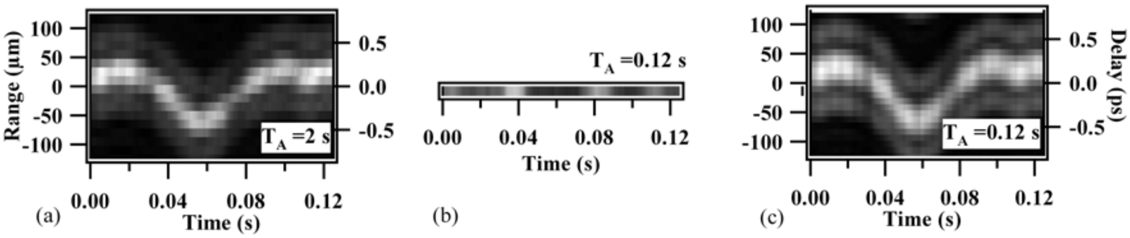

Fig. 2. Range image of the disk for one full rotation (0.12 sec), balanced signal and LO arms. The data are averaged over 10 ms. (a) Data from conventional system at 17 LO delays. (b) Conventional data for a fixed delay. (c) FReCL data at the same fixed delay. Zero padding smooths the image. T_A is the total acquisition time.

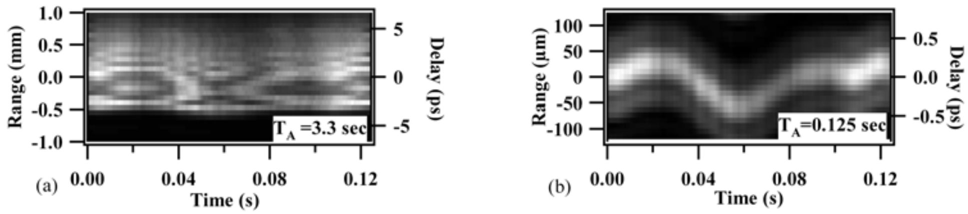

Fig. 3. Range image with 1 km of fiber in the signal path for (a) Conventional data at 27 delay steps of 0.5 ps each, and for (b) FReCL data at a fixed LO delay after phase compensation. Note the ~10x larger range scale in (a) versus (b).

Now consider the Doppler signal obtained by incoherently processing the FReCL data. If the target tilt provides sufficient range depth (> 250 μm) the N FReCL channels are decorrelated and incoherent summing can directly improve the SNR, as demonstrated in Fig 4a. Fig. 4b shows the resulting improvement in the measurement of a 50 Hz vibration. As expected, the FReCL data provide an N-times lower variance than do the conventional data.

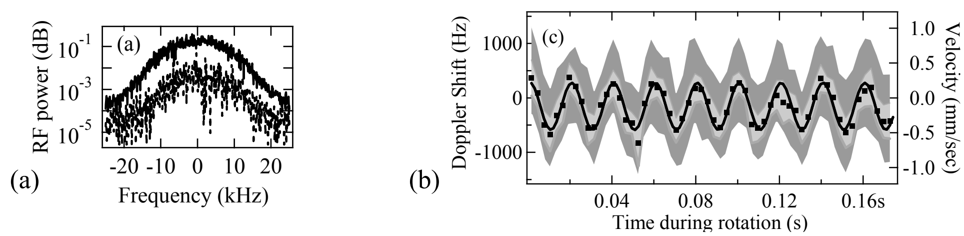

Fig. 4. (a) Doppler frequency spectrum of FReCL data (upper trace) and conventional data (lower trace) (b) Example vibration measurement showing truth data (solid line) and average of 120 speckle-decorrelated runs for the FReCL channel (solid squares). For a single measurement (one target rotation), the standard deviation for the FReCL data is 280 Hz (light grey region) and for the single conventional channel is 700 Hz (dark grey region).

References:

1. S. A. Diddams, D. J. Jones, S. T. C. J. Ye, J. L. Hall, J. K. Ranka, R. S. Windeler, R. Holzwarth, T. Udem, and T. W. Hänsch, "Direct Link between Microwave and Optical Frequencies with a 300 THz Femtosecond Laser Comb," Phys. Rev. Lett. 84, 5102 (2000).
2. B. R. Washburn, S. A. Diddams, N. R. Newbury, J. W. Nicholson, M. F. Yan, and C. G. Jørgensen, "Phase-locked erbium-fiber-laser-based frequency comb in the near infrared," Opt. Lett. 29, 250-252 (2004).
3. T. R. Schibli, K. Minoshima, F.-L. Hong, H. Inaba, A. Onae, H. Matsumoto, I. Hartl, and M. N. Fermann, "Frequency metrology with a turnkey all-fiber system," Opt. Lett. 29, 2467-2469 (2004).
4. K. Minoshima and H. Matsumoto, "High-accuracy measurement of 240-m distance in an optical tunnel by use of a compact femtosecond laser," Appl. Opt. 39, 5512-5517 (2000).
5. J. Ye, "Absolute measurement of long, arbitrary distance to less than an optical fringe," Opt. Lett. 29, 1153-1155 (2004).
6. W. C. Swann and N. R. Newbury, "Frequency-Resolved Coherent LIDAR using a Femtosecond Fiber Laser," Opt. Lett., to be published.
7. M. Wojtkowski, V. J. Srinivasan, T. H. Ko, J. G. Fujimoto, A. Kowalczyk, and J. S. Duker, "Ultrahigh-resolution, high-speed, Fourier domain optical coherence tomography and methods for dispersion compensation," Opt. Express 12, 2404-2422 (2004).
8. P. Drobinski, P. H. Flamant, and P. Salamitou, "Spectral diversity technique for heterodyne Doppler lidar that uses hard target returns," Appl. Opt. 39, 376-385 (2000).
9. K. D. Ridley, G. N. Pearson, and M. Harris, "Improved speckle statistics in coherent differential absorption lidar with in-fiber wavelength multiplexing," Appl. Opt. 40, 2017-2023 (2001).
10. B. R. Washburn, R. Fox, N. R. Newbury, J. W. Nicholson, K. Feder, P. S. Westbrook, and C. G. Jørgensen, "Fiber-laser-based frequency comb with a tunable repetition rate," Opt. Express 12, 4999-5004 (2004).